fermi
national accelerator laboratory

TM-542
0625.000

A PARTIAL-PRESSURE DRIFT CHAMBER BEAM INTENSITY MONITOR FOR EXTERNAL PROTON LINES

Fred Hornstra
Fermi National Accelerator Laboratory

January 3, 1975

Operated by Universities Research Association Inc. Under Contract with the United States Atomic Energy Commission

Introduction

As a replacement for SEM's (Secondary Emission Monitors), a D.C. beam monitor has been designed and operated in the extracted proton beam at the Fermilab accelerator. This monitor operates as a drift chamber in the partial pressure of the external beam line. The residual gas ions liberated by the incident proton beam drift transversely to a detector electrode and are measured. An independent measure of the ionization probability in the detector is provided by a Schulz/Phelps ionization "pressure" gauge. The ratio of the drift chamber signal to the ionization probability (as measured by the ionization "pressure" gauge) give slow spill relative intensity measurements. Reproducibility approaching one percent appear possible which is at least an order of magnitude better than that exhibited by our present SEM's. An additional advantage of this new detector is that D.C. beam intensity can be measured without introducing scattering material in the beam.

Secondary Emission Monitors (SEM's)

As the motivation to build this detector was primarily derived from deficiencies exhibited by SEM's, a brief description of these devices is appropriate.

A SEM is a beam intensity monitor having a number of thin foils traversed by the incident beam. Signal foils and high voltage foils are alternately interleaved in the chamber with a typical SEM having 10 signal foils and 11 high voltage foils. Whether electrons are emitted or collected by the signal foils is determined by the polarity of the high voltage foils which are operated at several hundred volts. Our SEM's are self contained in their own vacuum system having a pair of 2 mil stainless steel beam vacuum windows and an appended titanium ion pump maintaining a pressure $< (10)^{-8}$ Torr. The total amount of scattering material presented to the beam is approximately 0.114 g/cm^2. A 300 GeV proton has a probability of $\sim$ 0.05 per foil of generating a secondary electron. With ten signal foils, the total sensi-

tivity of a SEM is about 0.5 electron per proton which is adequate to measure $(10)^{10}$ protons with one percent resolution ($(10)^{8}$ protons per least count).

One beneficial aspect of a SEM is that it works well for slow or fast spill. The relative inefficient process of secondary electron production results in low space charge density even for large instantaneous beam currents. This feature makes it possible to calibrate the device with a beam torroid requiring a short high current burst of beam such as derived from single turn extraction from the accelerator.

Reproducibility is a problem, however. As secondary electron production is a surface phenomenon, changes in surface conditions have a marked effect on the performance of a SEM. The incident beam appears capable of changing the sensitivity. Where ~ $(10)^{19}$ protons have traversed a ~ $1cm^2$ area of the SEM, a localized sensitivity decrease of 20 percent has been observed. Evidence of this variation is presented as Figure 1 where the abscissa represents the beam position in the SEM as it was moved transverse to the incident proton beam. The ordinate represents the SEM response normalized to an upstream stationary reference SEM. The 20 percent dip in sensitivity occurs where the beam has resided for the past year. In contrast, it is interesting to note that an identically constructed SEM showed a localized 10 percent increase in sensitivity. The reason for this anomalous behavior is not understood. Clearly though, a change in beam position or a change in time results in a change in sensitivity, and calibration of such a device is valid only for a given beam position for a given instant of time.

These SEM's were fabricated by a commercial vendor who has supplied these devices to many laboratories.

The Partial-Pressure Drift Chamber Intensity Monitor

The deficiencies noted above and a desire to make a transparent low intensity DC beam intensity monitor led to the development of the partial-pressure drift chamber intensity monitor. The simple construction of the detector is illustrated in Figure 2. Depicted are the essential components which are the plate, the gradient wires, a grid, and a segmented detector surrounded by a guard ring.

The detector is installed in a vacuum pipe so that the beam travels near the center. Above the beam, the plate establishes the drift field which accelerates the liberated ions to the detector. The gradient wires at the side keep the field homogeneous in the body of the detector. The grid below the beam and above the signal electrode is biased to suppress secondary electrons generated at the signal electrode by the impinging ions. Enhancing the signal, these secondary electrons contribute only a few percent; however, to preclude a change in the detector surface conditions from effecting the sensitivity of the detector, the secondary electrons are largely suppressed by operating the grid a few volts negative with respect to the signal electrode. In this manner, the long term reproducibility of the detector is enhanced.

The guard ring serves to drain surface leakage currents harmlessly to ground. Also the guard is extended upstream and downstream a sufficient distance to eliminate fringe fields in the sensitive, or active, length of the detector.

The ion pick-up electrode is segmented with a center signal strip and two adjacent antisignal strips. The geometry of these may be chosen to fit the required active extent of the chamber. If the beam is transported cleanly, little or no signal is observed on the antisignal strips; however, when an upstream scattering source is present, the signal on these strips increases

in proportion to the observed increase on the signal strip. The actual signal from the detector is formed as follows:

$$s = s_a - \tfrac{1}{2} \frac{W_s}{W_{\bar{s}}} \bar{S} \qquad (1)$$

where

s = the corrected detector signal
s_a = the apparent signal on the center strip
$\bar{s}$ = the signal from the antisignal strips
W_s = the width of the center signal strip
$W_{\bar{s}}$ = the width of each antisignal strip
$\frac{1}{2} \frac{W_{\bar{s}}}{W_s} \equiv$ the antisignal weighting factor.

The function described in equation (1) is easily derived electronically. For the presently installed detector, $W_s = W_{\bar{s}} =$ 1 in., and the antisignal weighting factor = 0.5. The detector is physically about 1 meter in length with an active length of 0.7m.

Theoretical Sensitivity

The theoretical sensitivity of the above partial-pressure drift chamber intensity is derived. The following quantities were used in the derivation:

$$\left. \frac{1}{\rho_{air}} \frac{dE}{dX} \right/ \begin{matrix} \\ 300 \text{ GeV} \\ \text{Proton} \end{matrix} = 3.4 \text{ MeV g}^{-1} \text{ cm}^2 \qquad (2)$$

Energy required to produce a primary[1] ion pair = 90eV (3)

$$\rho_{air,\ 1atm} = 1.2\ (10)^{-3} \text{g cm}^{-3}. \qquad (4)$$

[1] At the pressures under consideration, secondary ionization is improbable as the mean free path is greater than the ion drift path; therefore, the 90 eV per primary ion pair is used in contrast to the oft quoted 30 eV per ion pair for gases near a pressure of 1 ATm or greater.

The number of ion pair is calculated per 300 GeV proton in an air pressure of 1 micron ($(10)^{-3}$Torr) for a detector 1 m long as follows:

$$\frac{\text{ion pair}}{(\text{proton})(\text{m})(\text{micron})} = \frac{\text{ion pair}}{\text{proton}(90\text{eV})} \cdot \frac{3.4(10)^{6}\text{eV cm}^2}{\text{g}} \cdot \frac{1.2(10)^{-3}\text{g}}{\text{cm}^3(760\text{Torr})} \cdot \frac{(100\text{cm})(10)^{-3}\text{Torr}}{\text{micron}}$$

$$= \frac{0.006 \text{ ion pair}}{\text{Proton micron (m)}}$$

At 10 microns the highest recommended pressure, the sensitivity of the 0.7 m long detector is as follows:

Sensitivity = (0.006)(10)(0.7) = 0.042 ion/proton which is about an order of magnitude less sensitivity than the SEM's described above. Operating at higher pressures for increased sensitivity is discouraged by the fact that at 10 microns, the mean free path is ~ 5.2 cm, a length which is approaching the drift path in the detector. At higher pressures, and shorter mean free paths, secondary multiplication can be expected.

Results

The performance of the drift chamber intensity monitor was checked against a calibrated SEM located downstream from the detector. The transverse beam size at this location is on the order of 0.5 cm. A SWIC (~ 0.05 g/cm^2) about 10 ft. upstream was used as a remotely insertable scattering source. A SWIC is typical of a

scattering source which might be introduced routinely in beam line operation.

Integration time extended over the entire one second extraction period. The detector signal was totalized on a 40 nf capacitor. This capacitor value is arbitrary and was used for convenience. At the end of the integration period, the analog voltage on the capacitor was digitized by a precision voltage to pulse train module having a transfer function of one pulse per millivolt.

In the data presented, beam rates ranged from $< (10)^{12}$ protons sec^{-1} to $\sim 8(10)^{12}$ protons $msec^{1}$, roughly a range of 4 decades. In some cases slow extraction of $\sim 5(10)^{12}$ protons for $\lesssim$ one sec was followed immediately by $\sim 5(10)^{12}$ protons in one millisecond. Beam rates above $8(10)^{12}$ protons $msec^{-1}$ gave an apparent enhanced sensitivity. No data is presented for this condition.

Figure 3 is a bias curve obtained while the detector operated in a constant pressure. The plate voltage was varied from zero to 500 volts as the ratio of the detector signals to the SEM were recorded. S_a is the signal from the center electrode and $\bar{s}$ the total antisignal from the adjacent antisignal electrodes. The grid was maintained at -10 volts.

The curves exhibit a plateau at approximately 200 volts with a slope of approximately one per cent per 100 volts. Later data has shown the plateau to be flat to a fraction of a percent above 600 volts.

Note that the antisignal, $\bar{s}$, without an upstream scattering source decreases to zero at a few volts and remains there. The transverse spread of the ions is obviously contained on the center electrode for the 0.5 cm beam size in the detector.

Another curve shows an apparent 2.5 percent increase in normalized signal when the upstream SWIC is inserted as a scattering

source. The corresponding 5 percent antisignal is also plotted. Application of equation 1 to obtain the corrected normalized signal is as follows:

$$S_n = 1.025 - \frac{(1)\ 1''\ \ (0.05)}{2\ \ 1''} = 1.0 \qquad (3)$$

Equation 3 and Figure 3 illustrate that the detector signal modified by the properly weighted antisignal compensates for this scattering source. An earlier experiment had showed that the reference SEM exhibited less than a one percent effect from this SWIC being in the beam.

Figure 4 shows the normalized detector response as the ionization probability varied over approximately an order of magnitude. The abscissas is the ionization probability in "microns" as measured with a Schulz/Phelps ionization "pressure" gauge. The ordinate is the detector response in ions per proton. The data for this figure were gathered over many weeks with various running conditions. The curve is a relatively straight line which extrapolates near the origin. Also in this figure is the theoretically calculated response curve. The observed response is only about six percent lower than that calculated above. The important feature of these data is the linearity of the "pressure" response which indicates that relatively large changes in "pressure" (ionization probability) are tolerable, provided that the detector signal is normalized to the ionization probability. The mean free path is also indicated on the abscissa showing that at an "ionization probability" of 10 microns, the mean free path is ~ 5 cm.

Discussion

In two respects, the partial-pressure drift chamber intensity monitor promises to be superior to a SEM. In two other ways a SEM remains superior. First the advantages of the drift chamber.

The long term reproducibility and stability should be superior for the drift chamber as no surface, which is subject to change in sensitivity, interacts with the beam. Only gas ions interact and these are always replenished; as a result, no beam position dependent sensitivity should be observable. Any drift in the ionization probability measurement (ion "pressure" gauge) would of course result in an apparent drift, but as long as the detector exhibits no position sensitivity change, occasional calibration checks may be meaningfully performed. A retractable SEM could perform this function. The stability of the SEM would be preserved by the fact that beam would rarely pass through the device.

The other superior feature of the drift chamber intensity monitor is that no material is added in the beam path. In many cases the pressure of the beam line is adequately high for the chamber to operate. In some cases lower pressure than that existing may be necessary resulting in a net reduction of material in the beam.

A SEM, however, has demonstrably better immunity to beam scattering sources. Although the antisignal strips in the drift monitor help compensate the effect, care should be taken to avoid larger sources of scattering than that from a SWIC.

For fast spill beam measurements, the SEM, at present, also is superior. The enhanced sensitivity of the drift chamber at beam rates approaching $(10)^{13}$ protons $msec^{-1}$ and above renders the detector deficient in this application. Work continues in understanding this phenomenon.

Conclusion

At the present state of development, the partial-pressure drift chamber intensity monitor should be a useful replacement for, or a supplement to, a SEM in beam lines where slow spill

only is used, and particularly where beam scattering by a SEM is a problem. Until more experience is gained with this detector, a retractable SEM should supplement as an intensity monitoring reference. Occasionaly, the SEM could be inserted into the beam for a few machine pulses to check the calibration. In this manner the stability and reproducibility of a SEM also would be preserved as rarely would beam pass through the device.

In beam lines where both slow and fast spill measurements are required, the drift chamber intensity monitor should be complimented with a beam torroid with each device gated to measure its respective spill.

Additional studies are required to understand the reason for the dramatic and abrupt enhanced sensitivity of the drift chamber for beam ratio approaching $(10)^{13}$ protons $msec^{-1}$. Work continues in this direction.

Acknowledgements

Many people deserve credit for help in the work which has proceded for the past few months. The operators gathered much data on the SEM's. Glenn Lee did the mechanical engineering on the drift detector, and Fred Larson and Ted Soszynski did the assembly. To Max Palmer and Larry Sauer goes a special thanks for modifying the vacuum septum in the Transfer Hall to accommodate this system.

And finally thanks to E. Bleser, H. Edwards, and E. Fisk for many interesting discussions and continual encouragement in the course of this undertaking and in the work which continues.

FH/emk

+800V

Figure 1

Normalized SEM Respon
Versus Beam Position

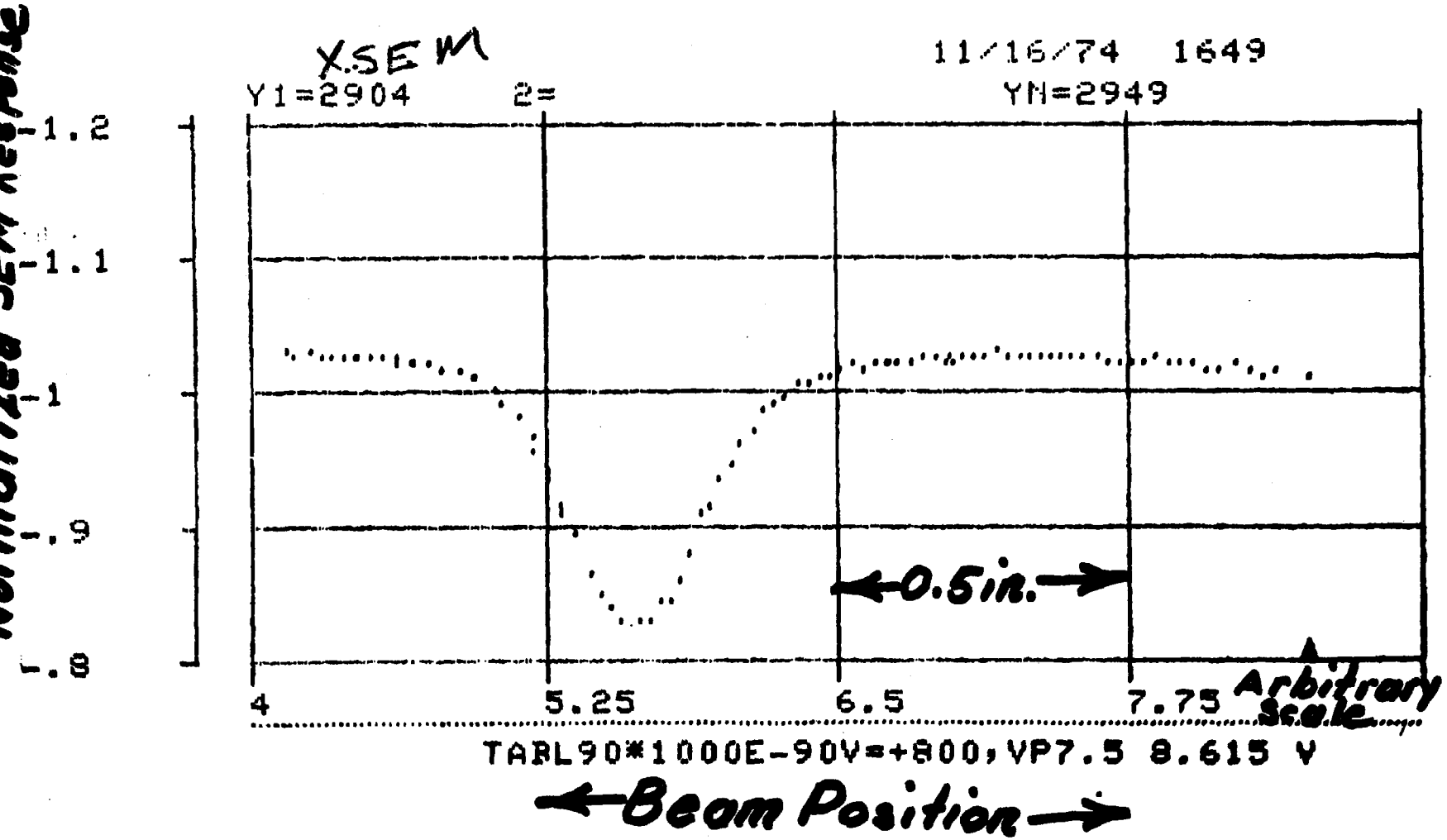

(Fig. 1)

TM-542

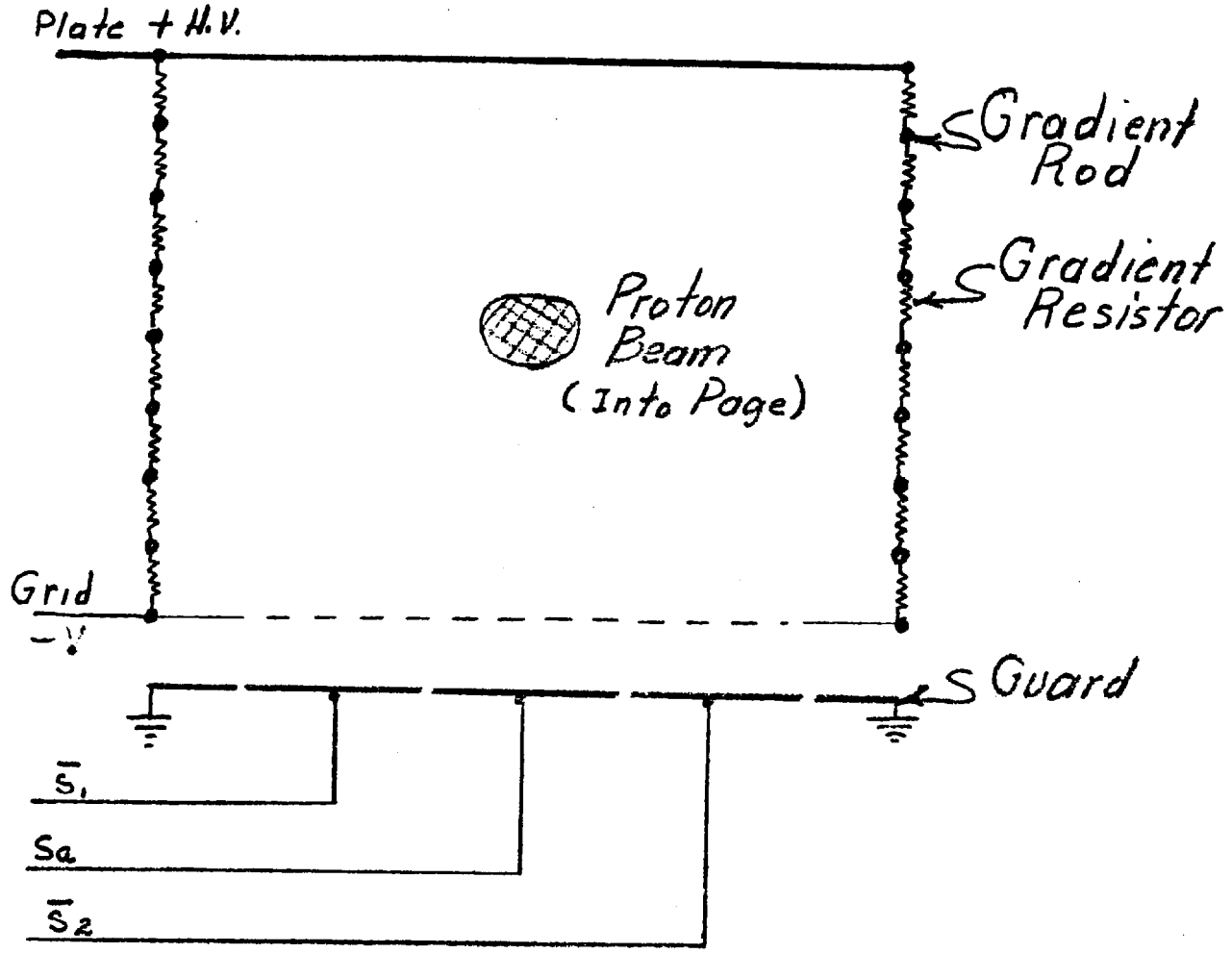

Figure 2
Partial-Pressure Drift Chamber
Intensity Monitor

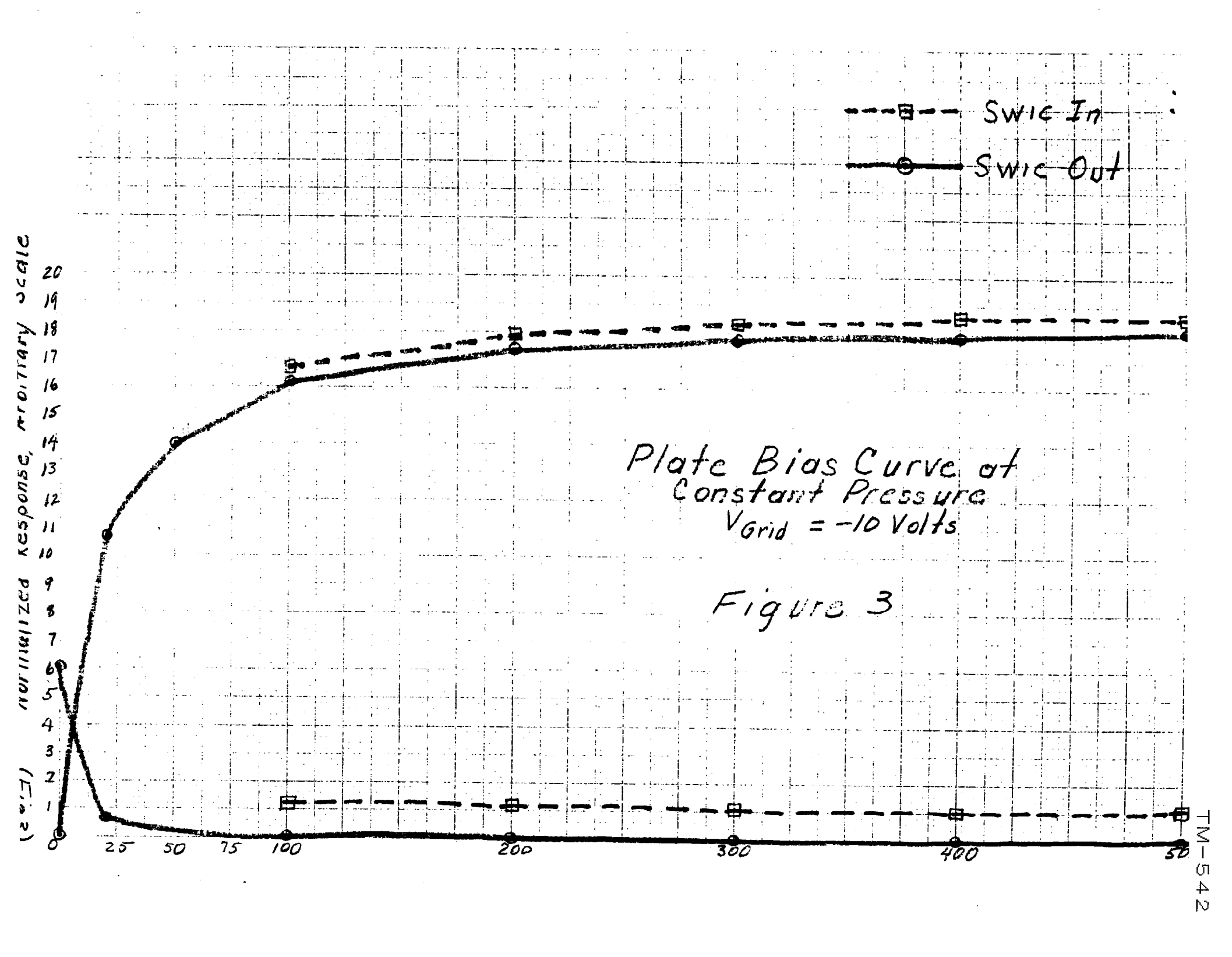
Swic In
Swic Out
Plate Bias Curve at
Constant Pressure
V_{Grid} = -10 Volts
Figure 3
Normalized response, arbitrary scale
(Ein)
0
25
50
75
100
200
300
400
500
1
2
3
4
5
6
7
8
9
10
11
12
13
14
15
16
17
18
19
20
TM-542

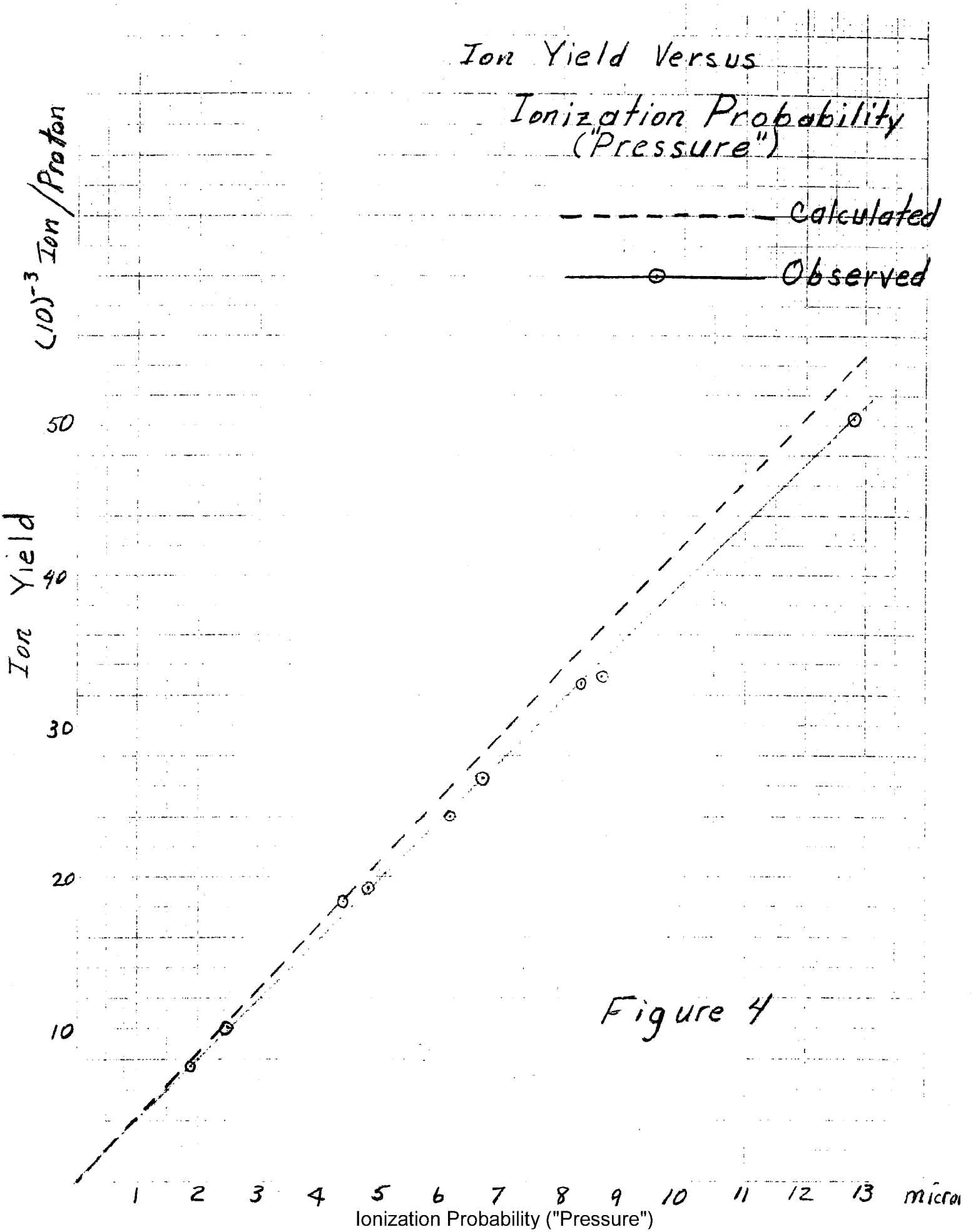
Ion Yield Versus
Ionization Probability
("Pressure")
Calculated
Observed
(10)$^{-3}$ Ion/Proton
Ion Yield
50
40
30
20
10
1
2
3
4
5
6
7
8
9
10
11
12
13
micron
Ionization Probability ("Pressure")

Figure 4

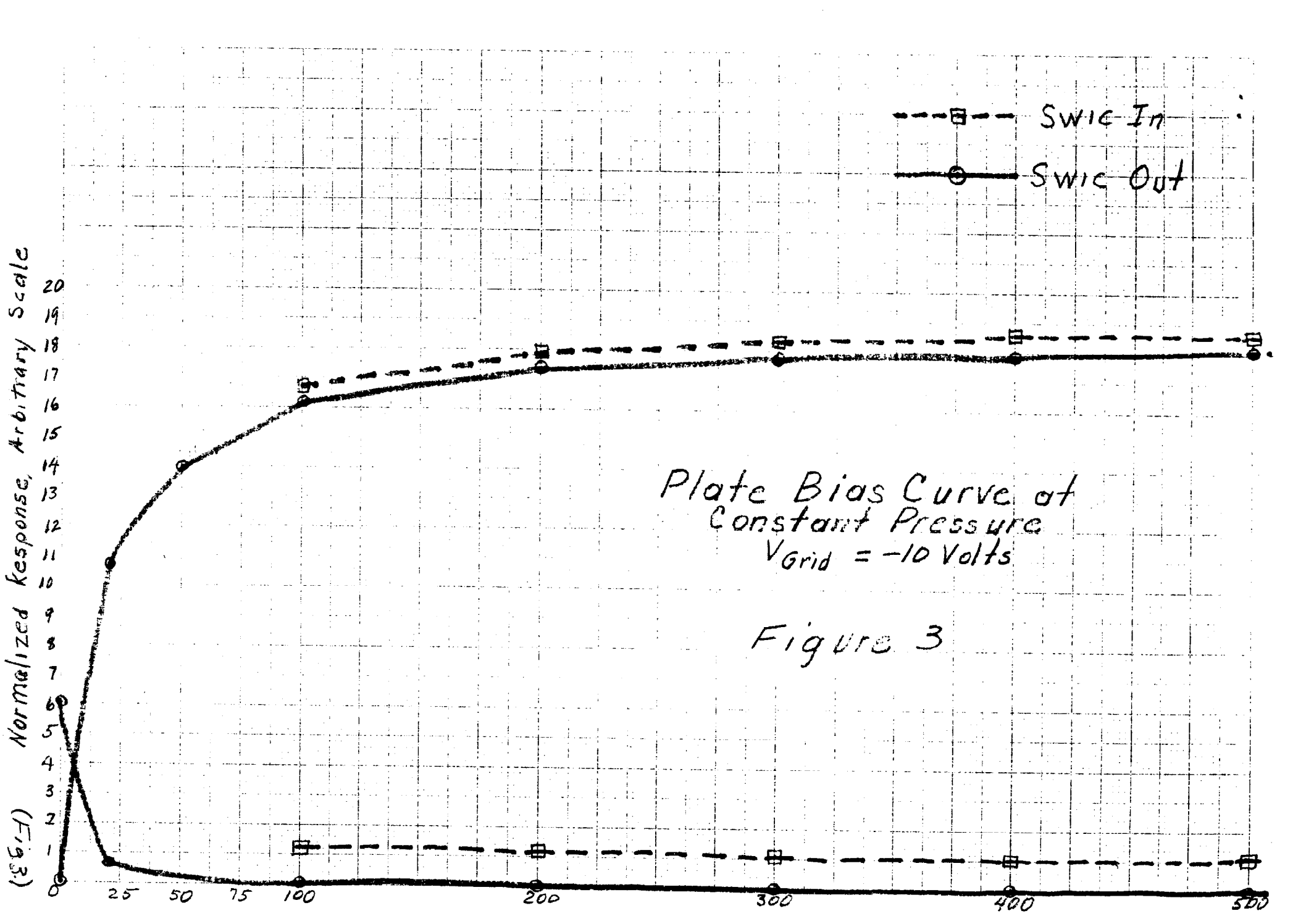

Plate Bias Curve at
Constant Pressure
$V_{Grid} = -10$ Volts

Figure 3

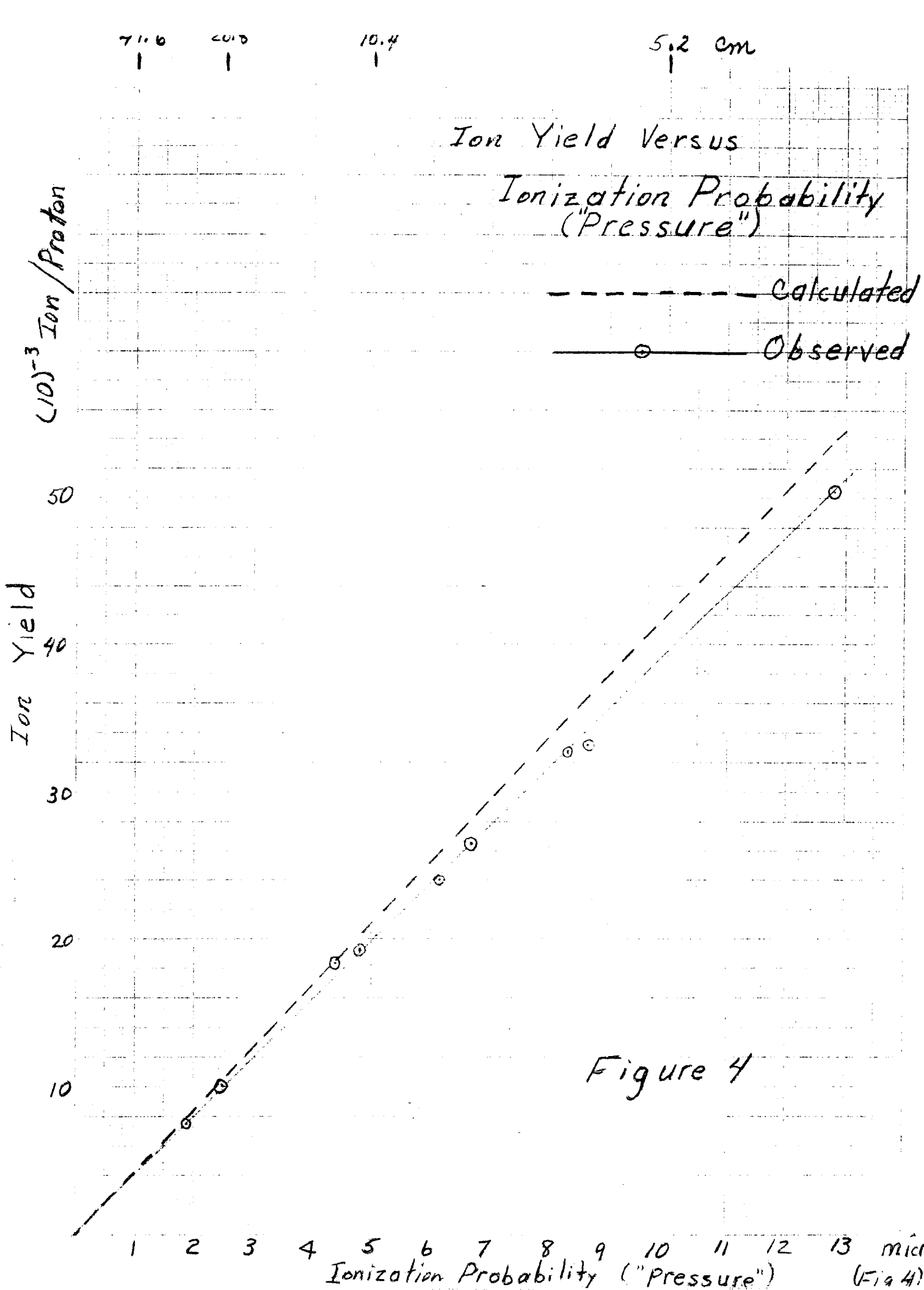

Figure 4

(Fig 4)